How Does Structural Disorder Impact Heterogeneous Catalysts? The Case of Ammonia Decomposition on Non-Stoichiometric Lithium Imide

Francesco Mambretti, Umberto Raucci, Manyi Yang, and Michele Parrinello*

Atomistic Simulations, Italian Institute of Technology, Genoa, Via Enrico Melen 83, GE 16153, Italy

E-mail: michele.parrinello@iit.it

Abstract

Among the many catalysts suggested for ammonia decomposition, Li_2NH has been shown to be quite promising. In the recent past, we have performed extensive *ab-initio*-quality simulations to explain the workings of this unusual catalyst. In the complex scenario that has emerged, surface dynamics and structural disorder enhanced by the interaction with the reacting ammonia molecules played a crucial role. Non-stoichiometric lithium imide $Li_{2-x}(NH_2)_x(NH)_{1-x}$ has been reported to have better catalytic performances than pure lithium imide. Stimulated by these findings, we follow up our first study simulating the ammonia decomposition on such non-stoichiometric compound. We attribute the enhanced reactivity to the fact that the compositional disorder further enhances the fluctuations in the topmost layers of the catalyst, strengthening our dynamical picture of this catalytic process.

The process of ammonia cracking involves its decomposition into nitrogen and hydrogen, and has recently attracted significant attention due to its potential as a hydrogen vector in a low-carbon economy .[1–5] Unlike H_2 itself, ammonia has the advantage that it can be easily liquefied and transported, making it an attractive alternative to direct hydrogen storage .[6] Furthermore, NH_3 has a lower cost per unit of stored energy, a larger volumetric energy density, an easier and already well-established widespread production, handling and distribution capacity, and better commercial viability .[3,7]

From an industrial perspective, the feasibility of H_2 production from ammonia crucially hinges on the development of efficient catalysts. Among the numerous suggestions made, lithium imide (Li_2NH) and, later, the imide-amide non stoichiometric compounds $Li_{2-x}(NH_2)_x(NH)_{1-x}$ have been found to have highly promising catalytic properties.[8–14] It has been argued that the catalytic performance of Li_2NH can be affected by the materials of the reactor, in particular transition metals such as nickel .[9,11] It is not clear whether the effect is additive,[11] or promotional.[9] However, it is not disputed that the non-stoichiometric compound has an enhanced activity .[10]

Progress in the construction of DFT-quality machine-learning-based reactive potentials [15–21] and the use of enhanced sampling techniques [22–26] to accelerate the occurrence of reactive events [27–32] have recently enabled the simulation of the ammonia decomposition process on pristine lithium imide .[33] This has allowed the catalytic mechanism of superionic Li_2NH to be unraveled and the key factors determining its activity to be unveiled. In particular, our simulations [28] have shown that surface imides quickly react with the incoming ammonia molecules, inducing the formation of a few diffusive almost liquid-like interfacial layers that act as a catalytic medium, promoting the complex steps that lead to the cracking of ammonia and the eventual release of N_2 and H_2 molecules. The catalytic efficiency of the activated Li_2NH surface results from its ability to store electrons in localized electronic states, exchange protons via Grotthuss-like mechanism and stabilize the different negative intermediates taking advantage of the screening provided by the mobile Li^+.

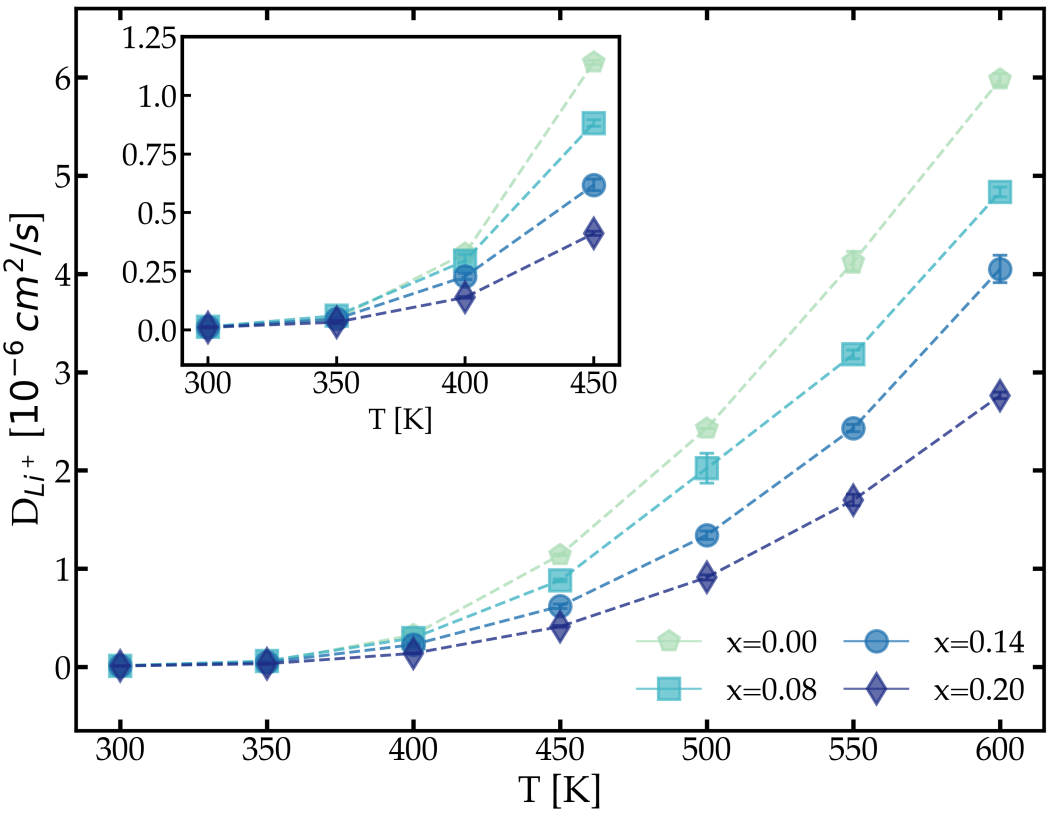

Figure 1: Temperature dependence of the lithium diffusion coefficient D_{Li^+} in the bulk. The NH_2^- concentrations simulated are $x = 0, 0.08, 0.14, 0.20$. Errorbars (almost always smaller than the symbol size) on each data point are computed as the standard deviation among three 6 ns-long simulations, each started from a different random arrangement of the amides. Inset: focus on $D_{Li^+}(x)$ between $T = 300$ K and $T = 450$ K.

Here, we use the same computational machinery based on machine learning potentials and enhanced simulation techniques (see Methods section), to study the imide-amide mixture $Li_{2-x}(NH_2)_x(NH)_{1-x}$, and to elucidate the origin of the reported enhanced catalytic performance .[8,10,12] We attribute this increased efficiency to the fact that the compositional disorder further facilitate the surface dynamical instability, thus supporting our interpretation of the Li_2NH catalytic activity.

Since superionicity in Li_2NH is key to its catalytic behavior, we started our investigation by studying the dependence of lithium cation diffusion coefficient D_{Li^+} on the amide concentration x (Fig. 1). At $x = 0$ the superionic behavior has been already experimentally

investigated ,[34,35] but no data for the mixtures are as yet available. However, it is comforting to find that in the pristine case there is a good agreement between theory and experiment as reported in Ref.[33]

As expected, at all concentrations studied D_{Li^+} increases as a function of temperature and around $\sim$ 350 K, as shown in the inset, D_{Li^+} grows by two orders of magnitude within a few tens of degrees, roughly indicating the onset of a superionic behavior. While lithium diffusion coefficient decreases as a function of x, at the *operando* temperature ($T > 500$K) it still remains large ($\sim 10^{-6}\,\mathrm{cm}^2/\mathrm{s}$), even for $x = 0.2$, which is the largest deviation from stoichiometry we have investigated. This concentration is sufficiently high for the amide effects to be important and for the mixture to remain stable.[10,11]

The presence of the amides in the mixture changes the surface dynamics by enhancing the fluctuations of the top layers with a magnitude that grows with x, even before the system is exposed to ammonia. In particular, NH_2^- groups in the top layer can be promoted to an adlayer, leaving behind vacancies (Figs. 2a and 2b). We quantified this effect in Fig. S1, where we analyzed the nitrogen density ρ_s^N in the surface layers. The data illustrate that an increase in the occupation number of the adlayer is concomitant with a slight reduction in the occupation of the two uppermost layers as the amide concentration increases. Furthermore, the presence of NH_2^- anions on the surface also favors imide-amide proton transfer reactions,[12,13,33,36–38] and inter-layer exchanges (see Figs. S2-S4 for statistical analyzes), which were not possible in the pure Li_2NH. This effect is clearly visible from the analysis of the spatial distribution of the N and Li atoms described by the probability $P_\alpha(z)$ (α =N, Li) of finding an atom of species α at a given value of the z coordinate (Figs. 2b) and 2d)). The distributions $P_N(z)$ in the first top layers broaden as x increases, corresponding to wider fluctuation of the amides in the top layer. Concurrently, lithium atoms move to balance the negative charge of amide groups, following a mechanism analogous to the one described in Ref.[33]

The first step in the ammonia decomposition process is the NH_3 absorption on the sur-

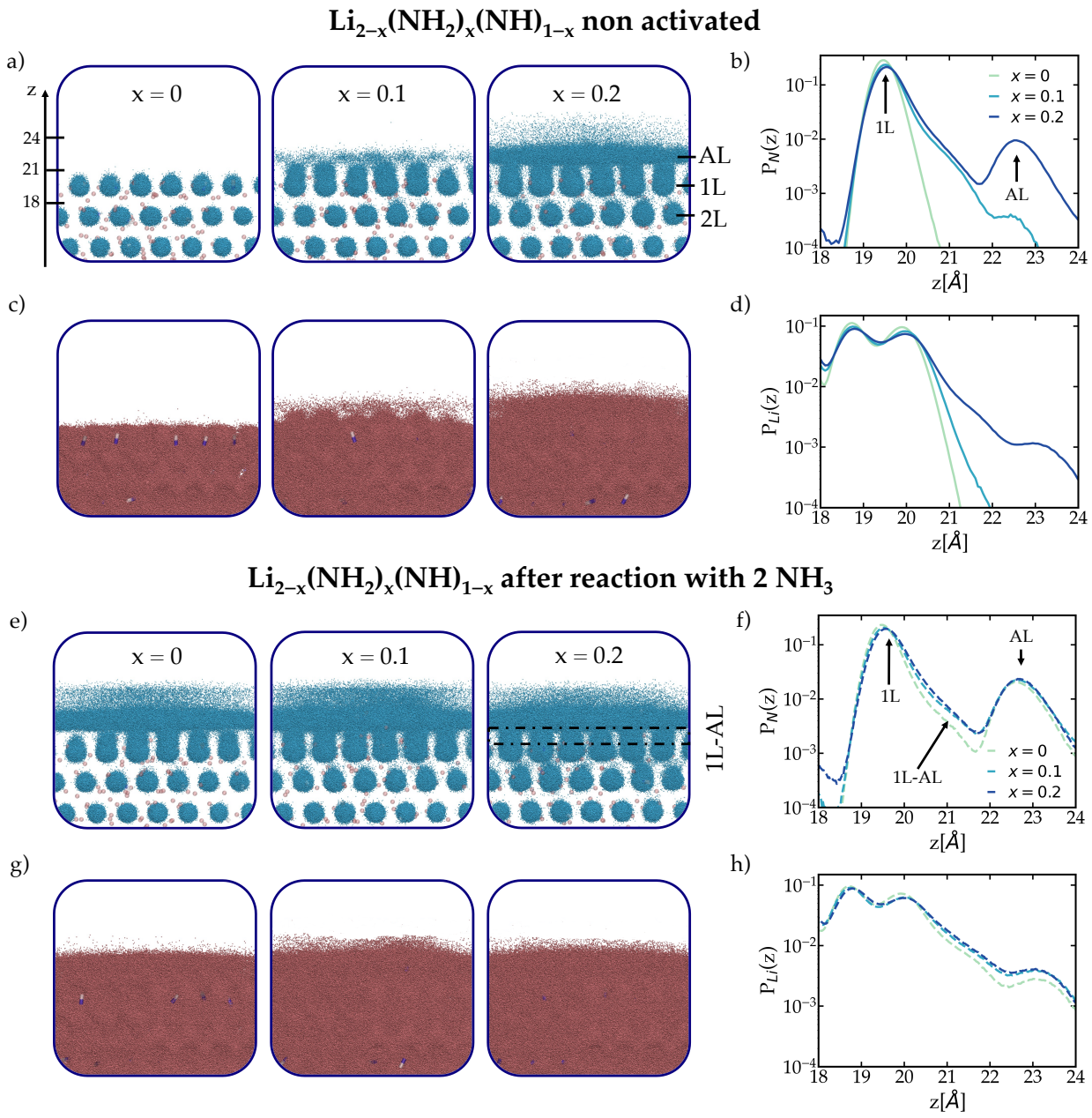

Figure 2: **a)** Scatter plot of the N atoms positions reported every 1ps, for $x = 0, 0.1, 0.2$, cumulated over four independent 30 ns-long trajectories, for a total time of 120 ns, before reaction with NH_3, at $T = 750$ K. To simplify reading, a single instantaneous configuration is chosen to represent Li atoms (pink). Labels 'AL','1L' and '2L' mark the adlayer, the first and the second layer, respectively. **b)** Probability $P_N(z)$ for N atoms to be found at a given z coordinate in the range [18,24] Å, at $x = 0, 0.1, 0.2$. Note the log scale on vertical axis. Peaks corresponding to first layer and adlayer are indicated. **c)** Same as panel a) but for Li atoms, with the corresponding $P_{Li}(z)$ distributions in panel d). Panels **e)**, **f)**, **g)** and **h)** are the same as panels a)-d), but after the reaction with two ammonia molecules. In panel e) and f), the intermediate region between 1L and AL is highlighted.

face, leading to the formation of two amide groups according to the proton transfer reaction NH_3+$NH^{2-} \rightarrow 2\ NH_2^-$, which takes place spontaneously on the nanosecond time scale. The ion distribution after absorption is analyzed in Figs. 2e-2h, from which one can visually assess that the addition of ammonia further enhances the fluctuations of the atoms in the topmost layers (Fig. S2-S6). After the surface is exposed to ammonia, the formation of the adlayer is only slightly dependent on x (Figs. S1, S2 and S5), with its average occupation reaching values in the range 15%-25% of the perfect crystal layer surface density (~ 0.09 Å^{-2}). Additionally, proton transfer reactions via Grotthuss-like mechanism are more abundant in this activated environment, and are proportional to the concentration of amides, taking place also for $x = 0$ (Figs. S3 and S6). The formation of other NH_2^- groups on the surface increases the inter-layer mobility. An example of this behaviour is shown in Fig. S4, where we tracked the z coordinate of an amide ion, which repeatedly jumps among the top layers. Furthermore, when a NH^{2-} transforms into a NH_2^-, this proton transfer makes it easier for the nitrogen to move from layer to layer (Fig. S3). These inter-layer movements are reflected by the height of the peaks of $P_N(z)$ and $P_{Li}(z)$ for the activated surface (Figs. 2f and S2).

After having analyzed the amplified surface fluctuations of the mixtures, we move to investigate the effect that these have on the catalytic activity of non-stoichiometric lithium imide. Thus, we focused on one of the key steps for ammonia reforming, namely, the formation of diazanediide in the reactive step NH^{2-}+ $NH^{2-} \rightarrow [HN\text{-}NH]^{2-} + 2e^-$.[33] Therefore, we computed the free energy surface (FES) for this reaction at different values x. In Fig. 3 the FES for the reaction in the first layer of the surface is reported as a function of the inverse distance $1/d_{AB}$ between the two nitrogen atoms N_A and N_B involved in the reaction, after the surface has been activated by the reagent ammonia. A similar profile for the diazanediide formation in the second layer is reported in Fig. S7, as well as the profiles obtained for the non activated surfaces (i.e., before ammonia absorption). It is seen that increasing the amides concentration leads to a systematically more stabilized diazanediide molecule. Furthermore, the barrier height $\Delta G^{\ddagger}$ diminishes as a function of the concentration

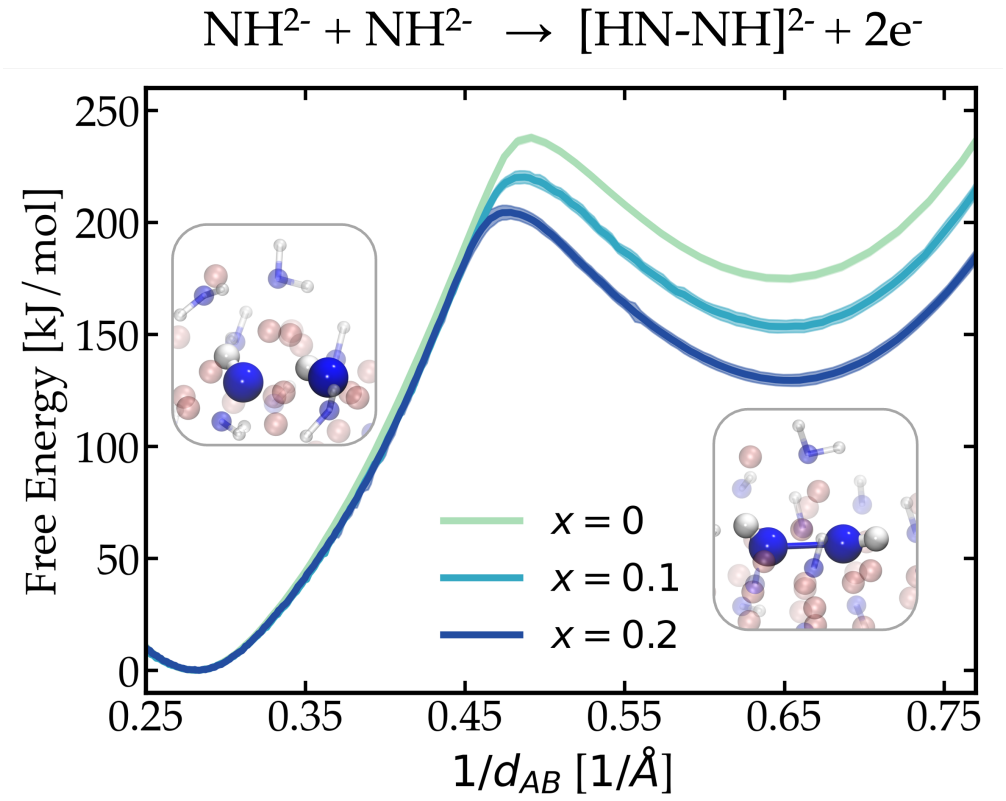

Figure 3: Free energy profiles computed from on-the-fly probability enhanced sampling (OPES)[23,24] simulations, for diazanediide formation from two imides in the first layer. The bias is applied to maximize the coordination number between the nitrogens N_A and N_B of a given pair of imides, whose distance is d_{AB}; here the horizontal axis reports $1/d_{AB}$ for clarity. The data shown in this picture have been obtained by cumulating the data coming from 4 independent 10 ns-long simulations, for each x value, for a total time of 40 ns. The reported errorbars are computed as the standard deviation among the 4 replicas. In each simulation with fixed x, a different pair of nitrogens has been biased, and also the initial configuration was different. The two insets show different snapshots from MD simulations with N_A and N_B being separated (left) or bonded to form diazanediide (right).

x, decreasing from ∼238 kJ/mol for x=0 to ∼204 kJ/mol in the mixture with 20% of amides. The electrons released during this reaction can be accommodated either in a diffuse surface state or in a localized state, similar to what happens in pure lithium imide (Fig. S8) .[33] Once formed, the diazanediide is stabilized by a cloud of Li^+ cations and it can eventually lead to a chain of reactions resulting in N_2 and H_2 formation. Given the increased number of amides, there is also another pathway to form the N-N bond, between an imide and an amide, with a subsequent abstraction of the excess hydrogen from $[HN\text{-}NH_2]^-$. Moreover, the reactions observed in Li_2NH are retrieved in lithium imide-amide mixtures (a full list is reported in the SI), with a catalytic cycle similar to the one we recently reported.[33]

In conclusion, our simulations highlight the crucial role played by the enhanced fluctuations of the surface in boosting the catalytic activity. The introduction of amide groups into the system induces increased structural disorder, resulting in a pronounced dynamical instability of the surface. This frustration manifests as amplified fluctuations, which are essential for promoting the catalytic reactions. This falls in line with the recent developments in heterogeneous catalysis that point to a highly relevant role of the surface disorder and dynamics.[29,33,39–41] Describing the surface dynamics in a statistical manner is, thus, fundamental for understanding the working principles of these catalysts and for identifying novel design strategies.

Acknowledgement

The authors thank Enrico Trizio for insightful discussions. This work was supported by funds from the AmmoRef project in the framework of the agreement between the Max Planck Institute and the Italian Institute of Technology (IIT). Computational resources were provided by the Swiss National Supercomputing Centre (CSCS) under project ID $S1134$ and $S1183$, by the IIT on the cluster Franklin and by CINECA via the IIT23_AtomSim_0 project.

Supporting Information Available

Additional results: nitrogen surface density, inter-layer jumps and atomic mobility, atomic displacements, proton transfer, diazanediide formation, F center, reactions discovered; Methods. Code and input files needed to replicate the simulations are deposited on the PLUMED-NEST repository.

References

(1) Schüth, F.; Palkovits, R.; Schlögl, R.; Su, D. S. Ammonia as a possible element in an energy infrastructure: catalysts for ammonia decomposition. *Energy Environ. Sci.* **2012**, *5*, 6278–6289.

(2) Cardoso, J. S.; Silva, V.; Rocha, R. C.; Hall, M. J.; Costa, M.; Eusébio, D. Ammonia as an energy vector: Current and future prospects for low-carbon fuel applications in internal combustion engines. *J. Clean. Prod.* **2021**, *296*, 126562.

(3) Valera-Medina, A.; Xiao, H.; Owen-Jones, M.; David, W.; Bowen, P. Ammonia for power. *Prog. Energy Combust. Sci.* **2018**, *69*, 63–102.

(4) Elishav, O.; Mosevitzky Lis, B.; Miller, E. M.; Arent, D. J.; Valera-Medina, A.; Grinberg Dana, A.; Shter, G. E.; Grader, G. S. Progress and Prospective of Nitrogen-Based Alternative Fuels. *Chem. Rev.* **2020**, *120*, 5352–5436, PMID: 32501681.

(5) Kobayashi, H.; Hayakawa, A.; Somarathne, K. K. A.; Okafor, E. C. Science and technology of ammonia combustion. *Proc. Combust. Inst.* **2019**, *37*, 109–133.

(6) Lucentini, I.; Garcia, X.; Vendrell, X.; Llorca, J. Review of the Decomposition of Ammonia to Generate Hydrogen. *Ind. Eng. Chem. Res.* **2021**, *60*, 18560–18611.

(7) Ravi, M.; Makepeace, J. W. Facilitating green ammonia manufacture under milder

conditions: what do heterogeneous catalyst formulations have to offer? *Chem. Sci.* **2022**, *13*, 890–908.

(8) Makepeace, J. W.; Jones, M. O.; Callear, S. K.; Edwards, P. P.; David, W. I. F. In situ X-ray powder diffraction studies of hydrogen storage and release in the Li–N–H system. *Phys. Chem. Chem. Phys.* **2014**, *16*, 4061–4070.

(9) Guo, J.; Wang, P.; Wu, G.; Wu, A.; Hu, D.; Xiong, Z.; Wang, J.; Yu, P.; Chang, F.; Chen, Z.; Chen, P. Lithium Imide Synergy with 3d Transition-Metal Nitrides Leading to Unprecedented Catalytic Activities for Ammonia Decomposition. *Angew. Chem. Int. Ed.* **2015**, *54*, 2950–2954.

(10) Makepeace, J. W.; Wood, T. J.; Hunter, H. M. A.; Jones, M. O.; David, W. I. F. Ammonia decomposition catalysis using non-stoichiometric lithium imide. *Chem. Sci.* **2015**, *6*, 3805–3815.

(11) Makepeace, J. W.; Hunter, H. M. A.; Wood, T. J.; Smith, R. I.; Murray, C. A.; David, W. I. F. Ammonia decomposition catalysis using lithium–calcium imide. *Faraday Discuss.* **2016**, *188*, 525–544.

(12) Makepeace, J. W.; David, W. I. F. Structural Insights into the Lithium Amide-Imide Solid Solution. *J. Phys. Chem. C* **2017**, *121*, 12010–12017.

(13) Makepeace, J. W.; Brittain, J. M.; Sukhwani Manghnani, A.; Murray, C. A.; Wood, T. J.; David, W. I. F. Compositional flexibility in Li-N-H materials: implications for ammonia catalysis and hydrogen storage. *Phys. Chem. Chem. Phys.* **2021**, *23*, 15091–15100.

(14) Guo, J.; Chen, P. Interplay of alkali, transition metals, nitrogen, and hydrogen in ammonia synthesis and decomposition reactions. *Acc. Chem. Res.* **2021**, *54*, 2434–2444.

(15) Behler, J.; Parrinello, M. Generalized neural-network representation of high-dimensional potential-energy surfaces. *Phys. Rev. Lett.* **2007**, *98*, 146401.

(16) Behler, J. Perspective: Machine learning potentials for atomistic simulations. *J. Chem. Phys.* **2016**, *145*, 170901.

(17) Behler, J. Four Generations of High-Dimensional Neural Network Potentials. *Chem. Rev.* **2021**, *121*, 10037–10072, PMID: 33779150.

(18) Miksch, A. M.; Morawietz, T.; Kästner, J.; Urban, A.; Artrith, N. Strategies for the construction of machine-learning potentials for accurate and efficient atomic-scale simulations. *Mach. learn.: sci. technol.* **2021**, *2*, 031001.

(19) Kocer, E.; Ko, T. W.; Behler, J. Neural Network Potentials: A Concise Overview of Methods. *Annu. Rev. Phys. Chem.* **2022**, *73*, 163–186, PMID: 34982580.

(20) Wang, H.; Zhang, L.; Han, J.; Weinan, E. DeePMD-kit: A deep learning package for many-body potential energy representation and molecular dynamics. *Comput. Phys. Commun.* **2018**, *228*, 178–184.

(21) Magdău, I.-B.; Arismendi-Arrieta, D. J.; Smith, H. E.; Grey, C. P.; Hermansson, K.; Csányi, G. Machine learning force fields for molecular liquids: Ethylene Carbonate/Ethyl Methyl Carbonate binary solvent. *Npj Comput. Mater.* **2023**, *9*, 146.

(22) Valsson, O.; Tiwary, P.; Parrinello, M. Enhancing Important Fluctuations: Rare Events and Metadynamics from a Conceptual Viewpoint. *Annu. Rev. Phys. Chem.* **2016**, *67*, 159–184, PMID: 26980304.

(23) Invernizzi, M.; Parrinello, M. Rethinking metadynamics: from bias potentials to probability distributions. *J. Phys. Chem. Lett* **2020**, *11*, 2731–2736.

(24) Invernizzi, M.; Piaggi, P. M.; Parrinello, M. Unified Approach to Enhanced Sampling. *Phys. Rev. X* **2020**, *10*, 041034.

(25) Bonati, L.; Trizio, E.; Rizzi, A.; Parrinello, M. A unified framework for machine learning collective variables for enhanced sampling simulations: mlcolvar. *J. Chem. Phys.* **2023**, *159*, 014801.

(26) Bussi, G.; Laio, A. Using metadynamics to explore complex free-energy landscapes. *Nat. Rev. Phys.* **2020**, *2*, 200–212.

(27) Yang, M.; Karmakar, T.; Parrinello, M. Liquid-liquid critical point in phosphorus. *Phys. Rev. Lett.* **2021**, *127*, 080603.

(28) Yang, M.; Bonati, L.; Polino, D.; Parrinello, M. Using metadynamics to build neural network potentials for reactive events: the case of urea decomposition in water. *Catalysis Today* **2022**, *387*, 143–149, 100 years of CASALE SA: a scientific perspective on catalytic processes.

(29) Bonati, L.; Polino, D.; Pizzolitto, C.; Biasi, P.; Eckert, R.; Reitmeier, S.; Schlögl, R.; Parrinello, M. Non-linear temperature dependence of nitrogen adsorption and decomposition on Fe (111) surface. *ChemrXiv* **2023**,

(30) Bonati, L.; Parrinello, M. Silicon liquid structure and crystal nucleation from *ab initio* deep metadynamics. *Phys. Rev. Lett.* **2018**, *121*, 265701.

(31) Zeng, J.; Cao, L.; Xu, M.; Zhu, T.; Zhang, J. Z. H. Complex reaction processes in combustion unraveled by neural network-based molecular dynamics simulation. *Nat. Comm.* **2020**, *11*, 5713.

(32) Xingyi, G.; Joseph, H.; Taehee, K.; Chao, Y.; Teresa, H.-G. Beyond potential energy surface benchmarking: a complete application of machine learning to chemical reactivity. *arXiv - PHYS - Chemical Physics* **2023**,

(33) Yang, M.; Raucci, U.; Parrinello, M. Reactant-induced dynamics of lithium imide surfaces during the ammonia decomposition process. *Nat. Catal.* **2023**,

(34) Li, W.; Wu, G.; Xiong, Z.; Feng, Y. P.; Chen, P. Li+ ionic conductivities and diffusion mechanisms in Li-based imides and lithium amide. *Phys. Chem. Chem. Phys.* **2012**, *14*, 1596–1606.

(35) Paik, B.; Wolczyk, A. Lithium imide (Li_2NH) as a solid-state electrolyte for electrochemical energy storage applications. *J. Phys. Chem. C* **2019**, *123*, 1619–1625.

(36) Miceli, G.; Ceriotti, M.; Bernasconi, M.; Parrinello, M. Static disorder and structural correlations in the low-temperature phase of lithium imide. *Phys. Rev. B* **2011**, *83*, 054119.

(37) Miceli, G.; Bernasconi, M. First-Principles Study of the Hydrogenation Process of Li2NH. *J. Phys. Chem. C* **2011**, *115*, 13496–13501.

(38) Miceli, G.; Ceriotti, M.; Angioletti-Uberti, S.; Bernasconi, M.; Parrinello, M. First-Principles Study of the High-Temperature Phase of Li2NH. *J. Phys. Chem. C* **2011**, *115*, 7076–7080.

(39) Tripathi, S.; Bonati, L.; Perego, S.; Parrinello, M. How poisoning is avoided in a step of relevance to the Haber-Bosch catalysis. *ChemrXiv* **2023**,

(40) Spencer, M. Stable and metastable metal surfaces in heterogeneous catalysis. *Nature* **1986**, *323*, 685–687.

(41) Schlögl, R. Heterogeneous catalysis. *Angewandte Chemie International Edition* **2015**, *54*, 3465–3520.

TOC Graphic